

Bayesian Methods for Multi-Objective Optimization of Hybrid Numerical Filters in ECG Signal Processing for Accurate Arrhythmia Classification

Zakaria Khatar^{1,*}, Dounia Bentaleb², Saadia Drissi³

¹*Superior School of Technical Education, University Hassan II, Morocco*

²*Faculty of Science Techniques, University Hassan II, Morocco*

³*Pluridisciplinary Laboratory of Research Innovation (LPRI), EMSI, Casablanca, Morocco*

Abstract This study introduces an innovative method for ECG signal processing that combines advanced filtering techniques, multi-objective Bayesian optimization, and a sophisticated deep learning architecture for classification. The methodology starts with Enhanced Empirical Mode Decomposition (EEMD) to break down the ECG signal into Intrinsic Mode Functions (IMFs). These IMFs undergo filtration through a series of Chebyshev Type II, Butterworth, Daubechies Wavelet, and Savitzky-Golay filters. To achieve optimal performance, a Bayesian multi-objective optimization strategy, augmented by reinforcement learning for dynamic weight adjustment and Gaussian process minimization, is utilized to fine-tune filter parameters. This process ensures maximum noise reduction while maintaining signal integrity. The optimized signals are then processed by an advanced deep learning architecture that includes parallel and residual connections, bidirectional GRU layers, and dense classification layers, enabling precise classification of cardiac conditions. The model's performance was rigorously tested across 12 different ECG leads, showing remarkable improvements in classification accuracy (ACC), sensitivity (SNS), and F1 score. Post-optimization results achieved impressive values of 99.24% for ACC, 99.04% for SNS, and 99.05% for F1 score, demonstrating the significant enhancement in ECG signal analysis and diagnostic reliability provided by the proposed approach.

Keywords Arrhythmia Classification, ECG Classification, Cardiovascular diseases Classification, ECG Signal Denoising, ECG Deep Learning Classification, Cardiac diseases classification

AMS 2010 subject classifications 68Q25, 68Q32, 68U20, 68T10

DOI: 10.19139/soic-2310-5070-2272

1. Introduction

The accurate classification of cardiac diseases is essential for effective diagnosis, as these conditions have a profound impact on global health. Cardiovascular diseases (CVDs) represent a significant public health concern and are among the leading causes of death worldwide [55]. Early detection and continuous monitoring are crucial for the effective management and successful treatment of these diseases. The electrocardiogram (ECG) is a pivotal non-invasive diagnostic tool that records the electrical activity of the heart, providing detailed insights into various cardiac pathologies and aiding in their identification and treatment [48, 49, 47, 56]. However, the reliability and effectiveness of ECGs can be compromised by noise. Common sources of noise in ECG signals include power line interference, muscle artifacts from non-cardiac muscles, and baseline wander caused by patient movements or breathing [57]. These noise elements can obscure the true ECG signal, leading to potential misinterpretation and misdiagnosis [50].

*Correspondence to: Dounia Bentaleb (Email: douniabentaleb@gmail.com). Faculty of Science Techniques, University Hassan II, Morocco.

Significant research has focused on denoising ECG signals, with advancements in signal processing techniques aimed at enhancing ECG signal quality while preserving diagnostic information. These methods range from traditional filtering techniques to advanced approaches utilizing machine learning and deep learning [59]. The goal is to develop algorithms that can effectively remove noise without distorting the essential cardiac information [52, 53, 58]. As the field of ECG signal processing progresses, there is a growing emphasis on developing robust and efficient denoising methods. These methods are critical to ensuring the reliability of ECG-based diagnostics and monitoring, ultimately contributing to improved cardiovascular health [60, 64]. Continued research and innovation in this area promise to enhance the accuracy and reliability of ECG analysis, facilitating more effective detection and management of cardiovascular diseases [54, ?].

In this paper, Section 2 provides a General Proposed Model Overview, outlining the overall framework of our approach and detailing the datasets employed in our study. In Section 3, we introduce our Proposed Filtration Model, which includes multiple advanced filtering techniques: enhanced empirical mode decomposition (EEMD), Chebyshev Type II filters, Butterworth, Daubechies Wavelet, and Savitzky-Golay filters, all designed for efficient noise reduction. Section 4 delves into the Bayesian Multi-Objective Optimization of Filter Parameters. This section covers our multi-criteria optimization approach, which uses cross-correlation and mean squared error (MSE) metrics to refine the filtration model for improved signal quality. Subsections include the optimization process, efficacy quantification, detailed multi-objective optimization methodology, optimization results, performance metrics evaluation, and signal visualizations. In Section 5, we present our Proposed Combined Deep Learning Architecture for Classification. This section describes our deep learning framework, which employs residual and parallel processing to accurately classify cardiac conditions such as arrhythmia and myocardial infarction. Section 6 provides the Results and Discussion, offering a comprehensive analysis of our model's performance. It includes a comparative analysis and visual analysis of performance, highlighting significant improvements in classification accuracy. Finally, Section 7 concludes the paper with a summary of our findings and suggests potential avenues for future research in the field of biomedical signal processing.

2. Literature Review

Recent progress in the field of ECG signal denoising has led to the development of various innovative techniques aimed at improving signal quality and diagnostic accuracy. These advancements span a wide range of methodologies, from deep learning approaches to advanced signal processing techniques.

In the realm of deep learning, several groundbreaking methods have emerged. Zhang et al. (2023) introduced a combination of Efficient Channel Attention (ECA-Net) and CycleGAN, demonstrating enhanced denoising performance [26]. Adversarial deep learning techniques have been explored by Mvuh et al. (2024) [30], while Wang et al. (2022) utilized conditional generative adversarial networks (CGANs) for ECG denoising [31]. More recently, Wang et al. (2023) proposed a deep convolutional generative adversarial network (GAN) with LSTM, showing significant potential in complex denoising scenarios [39]. Hou et al. (2023) developed deep neural networks utilizing sparse representation algorithms for ECG signal denoising [41]. Additionally, Huang et al. (2023) introduced a portable detection system using bidirectional LSTM and residual blocks for automatic arrhythmia detection [44].

Advanced signal decomposition and filtering techniques have also seen significant advancements. Hossain et al. (2020) developed a variable frequency complex demodulation technique for precise noise reduction [27]. Mir et al. (2023) proposed a hybrid approach merging variational mode decomposition with empirical wavelet transform [29]. Singh et al. (2017) introduced a modified empirical mode decomposition (EMD) method [32]. Khatar et al. (2024) made significant strides in cardiac arrhythmia detection by introducing a model combining deep learning with a three-stage filter incorporating Chebyshev, Butterworth, and Daubechies wavelets, along with multi-scale signal analysis [24, 2].

Other notable contributions include the development of an adaptive Kalman filter bank by Hesar et al. (2020) [36], methods based on stationary wavelet transform by Kumar et al. (2020) [37], and innovative filtering techniques

using optimization algorithms for improved decomposition by Malghan et al. (2022) [46]. Parah et al. (2023) introduced iterative filtering combined with lifting wavelet transform for effective noise elimination [45].

Novel filtering and optimization approaches have also been explored. Sarafan et al. (2022) presented an ECG denoising technique using the Ensemble Kalman Filter [40]. Boda et al. (2021) proposed a hybrid method combining empirical mode decomposition (EMD) and empirical wavelet transform (EWT) to effectively eliminate power line interference and baseline wander [42]. Mourad (2022) introduced an ECG denoising approach based on successive local filtering [43], while Trigano et al. (2023) developed an adaptive trend filtering method for ECG denoising and delineation [28].

Further advancements include a low-distortion adaptive Savitzky-Golay filter based on discrete curvature estimation by Huang et al. (2019) [33], an integrated EMD adaptive threshold denoising method by Zhang and Wei (2020) [34], and an adaptive Fourier decomposition-based ECG denoising method by Wang et al. (2016) [35].

Some researchers have focused on addressing specific challenges in ECG signal processing. Souriau et al. (2022) applied dynamic time warping for fetal ECG denoising [38], addressing the unique challenges in prenatal cardiac monitoring. Li et al. (2022) proposed a novel approach combining wavelet transform and adaptive filtering for motion artifact removal in ECG signals [62]. Zhao et al. (2021) introduced a method using variational mode decomposition and correlation analysis for ECG denoising in wearable devices [63].

The field of ECG signal processing continues to evolve rapidly, with a growing interest in combining traditional signal processing techniques with advanced machine learning methods. There is also an increasing focus on real-time processing and implementation of these algorithms in portable devices. These collective efforts in ECG denoising research emphasize a strong commitment to enhancing the reliability and accuracy of cardiovascular disease diagnostics. Advances in signal processing and machine learning not only promise improved diagnostic capabilities but also pave the way for more sophisticated healthcare technologies.

3. General Proposed Model Overview

This paper introduces an innovative approach to ECG signal processing, which includes three main components: signal filtration, parameter optimization, and classification. Each component is designed to address specific challenges and enhance the overall performance of ECG signal analysis.

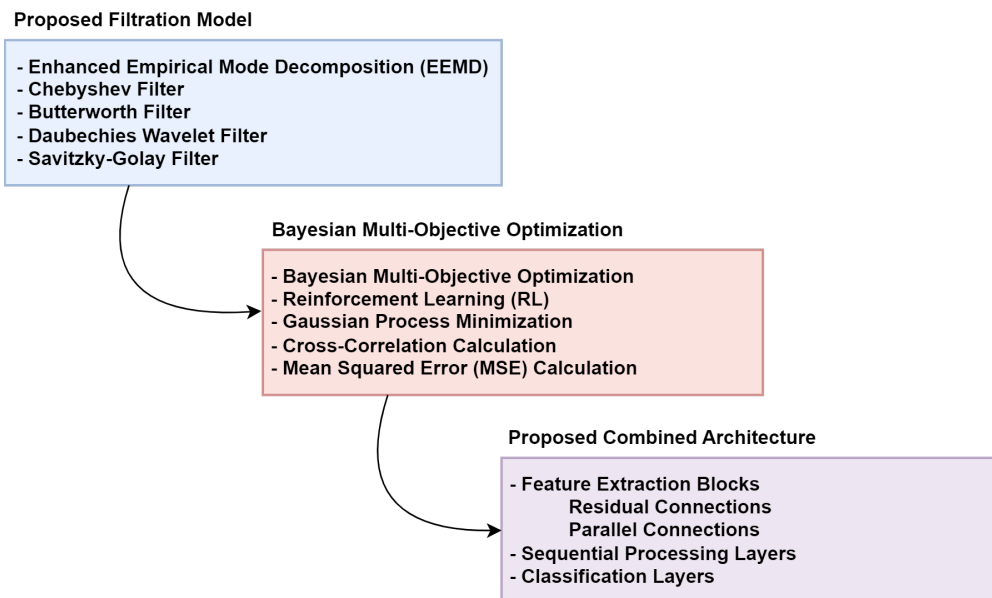


Figure 1. General process flow of the proposed ECG signal filtration, optimization, and classification model.

The general process flow of the proposed model is depicted in Figure 1. The process begins with the filtration stage, where the raw ECG signal undergoes several advanced filtering techniques to reduce noise and preserve essential signal characteristics. Following this, the Bayesian multi-objective optimization stage fine-tunes the filter parameters to maximize noise reduction while maintaining signal fidelity. Finally, the optimized signals are processed through an advanced deep learning architecture for accurate classification of cardiac conditions.

The subsequent sections will detail each of these components: - The **Proposed Filtration Model** employs Enhanced Empirical Mode Decomposition (EEMD) followed by a series of filters including Chebyshev Type II, Butterworth, Daubechies Wavelet, and Savitzky-Golay filters. - The **Bayesian multi-objective optimization** approach incorporates reinforcement learning (RL) for dynamic weight adjustment, Gaussian process minimization, and calculates metrics such as cross-correlation and mean squared error (MSE) to evaluate filter performance. - The **Proposed Combined Architecture** consists of feature extraction blocks, sequential processing layers including bidirectional GRU units, and classification layers with dense and softmax functions to accurately identify cardiac anomalies.

Each stage is crucial for the overall efficacy of the ECG signal analysis, contributing to improved diagnostic accuracy and reliability.

3.1. Datasets Employed

To conduct our study on cardiac arrhythmia detection and classification, we leveraged the MIT-BIH Arrhythmia Database. This database is highly esteemed in the field of electrocardiogram (ECG) research due to its extensive and meticulously annotated collection of ECG recordings. The database encompasses a wide variety of arrhythmia types, providing a robust and comprehensive resource that is essential for training and evaluating deep learning models. The diversity and detailed annotations of the MIT-BIH Arrhythmia Database facilitate the accurate identification and classification of multiple types of cardiac arrhythmias, thereby significantly contributing to the reliability and effectiveness of our model [69].

4. Proposed Filtration Model

This paper introduces a comprehensive approach to ECG signal processing by integrating multiple advanced techniques. Each technique is meticulously chosen for its effectiveness in mitigating specific challenges inherent to ECG signals, which are typically burdened with noise and artifacts due to their non-linear and non-stationary nature. The harmonious integration of these techniques is designed to achieve effective denoising while preserving the crucial characteristics of the ECG signal, thereby enhancing its diagnostic value. Our innovative model design and the seamless integration of these diverse techniques signify a significant advancement in biomedical signal processing.

The process flow of our model is depicted in Figure 2. It begins with the input ECG signal undergoing Enhanced Empirical Mode Decomposition (EEMD) to extract the Intrinsic Mode Functions (IMFs). Each IMF is subsequently processed through a sequence of filters—Chebyshev Type II, Butterworth, Daubechies Wavelet, and Savitzky-Golay—to reduce noise while maintaining the integrity of the signal's features. The filtered IMFs are then combined to yield a denoised ECG signal ready for diagnostic evaluation. This staged approach is crafted to tackle various types of noise and artifacts while preserving the signal's integrity.

In the following sections, we describe each component represented in the diagram and elaborate on their respective roles in the signal processing chain.

4.1. Empirical Mode Decomposition (EEMD)

Central to our model is the Enhanced Empirical Mode Decomposition (EEMD), which addresses the mode-mixing issue associated with classical EMD. EEMD is particularly effective for non-linear and non-stationary signals such as ECGs, decomposing them into Intrinsic Mode Functions (IMFs). Each IMF represents a simple oscillatory mode, simplifying subsequent signal analysis. EEMD serves as the foundational step in the signal purification process, breaking down the ECG into manageable components.

$$\text{Signal} = \sum_{n=1}^N \text{IMF}_n + \text{Residue} \tag{1}$$

Here, IMF_n denotes the n -th intrinsic mode function, and the residue represents the part of the signal that remains undecomposed into IMFs. The combination of these IMFs, along with the residue, reconstructs the original ECG signal, now ready for further refinement.

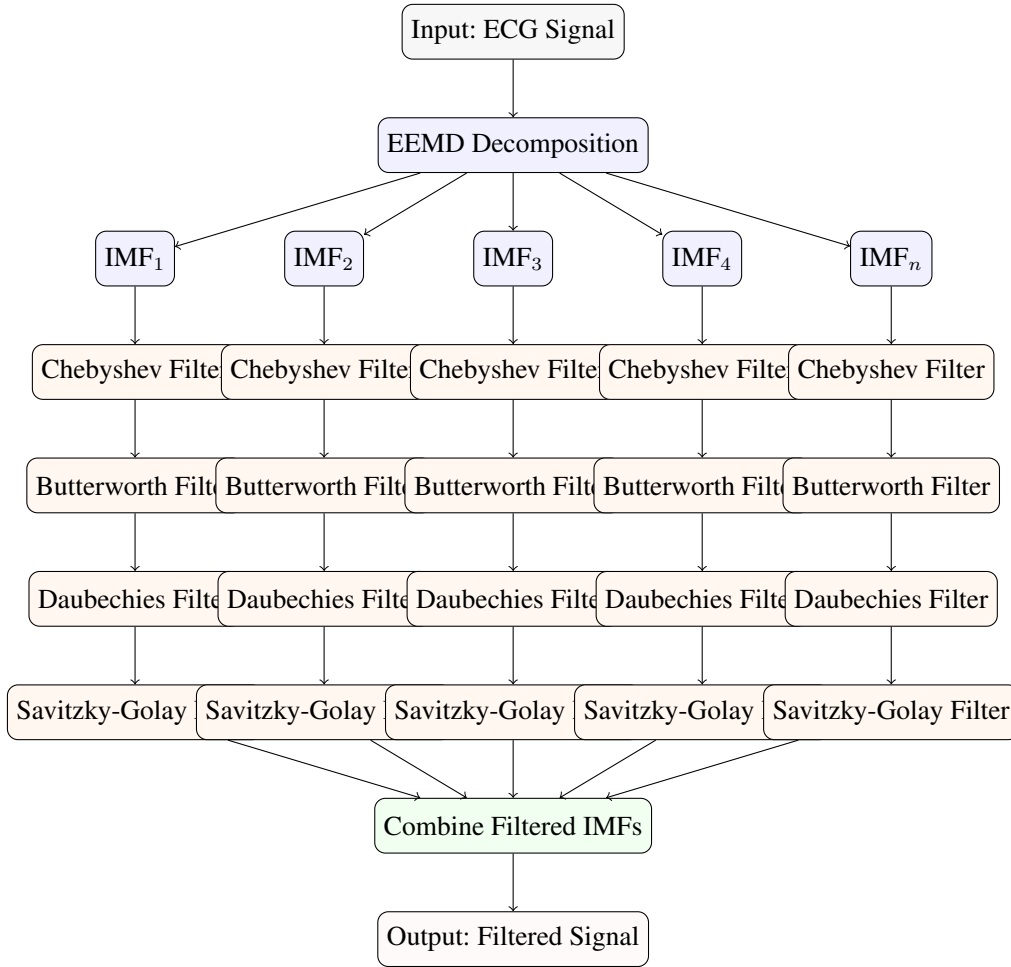


Figure 2. Diagram of the different Filtration Stages in the Proposed Model.

4.2. Chebyshev Type II Filter

After EEMD, the Chebyshev Type II Filter is applied. This filter is chosen for its rapid attenuation beyond the passband, essential for minimizing distortions within the frequencies of interest. It effectively reduces noise while maintaining the integrity of the ECG waveform.

$$H(f) = \frac{1}{\sqrt{1 + \varepsilon^2 T_n^2 \left(\frac{f}{f_c} \right)}} \tag{2}$$

In this expression, $H(f)$ represents the filter’s transfer function, where ε is the ripple factor in the stopband, T_n is the n -th Chebyshev polynomial, and f_c is the filter’s cutoff frequency.

4.3. Butterworth Filter

Concurrently with the Chebyshev filter, the Butterworth Filter, known for its flat frequency response, is employed to minimize distortion within the passband. This characteristic is crucial for preserving the fidelity of the ECG signal, ensuring that critical cardiac events are accurately represented.

$$H(f) = \frac{1}{\sqrt{1 + \left(\frac{f}{f_c}\right)^{2n}}} \quad (3)$$

The transfer function $H(f)$ of the Butterworth filter is shown here, with f_c being the cutoff frequency and n the order of the filter, determining the steepness of the frequency response at the cutoff.

4.4. Daubechies Wavelet Filter

The Daubechies Wavelet Filter is used to capture both the frequency and temporal characteristics of the IMFs, a vital step in identifying and correcting non-stationary components within the ECG signal. This dual capability ensures that our model is sensitive to the subtle yet diagnostically significant nuances of the cardiac signal.

$$\text{Signal} = \sum_j \left(\sum_k d_{j,k} \psi_{j,k}(t) \right) + a_J \phi(t) \quad (4)$$

In this equation, $d_{j,k}$ denotes the wavelet coefficients at scale j and position k , $\psi_{j,k}(t)$ are the Daubechies wavelet functions, and a_J is the scaling coefficient at the coarsest scale J , with $\phi(t)$ being the associated scaling function.

4.5. Savitzky-Golay Filter

Finally, the Savitzky-Golay Filter is implemented for its ability to smooth the IMFs, reducing noise while preserving important features such as peaks and troughs, which are crucial for the analysis of ECG signals. This filter is the final step in our multi-stage signal refinement process.

$$y'_i = \sum_{j=-m}^m c_j y_{i+j} \quad (5)$$

In the equation above, y'_i is the smoothed signal value, y_{i+j} are the input signal values, and c_j are the filter coefficients determined by polynomial regression, with m being the half-width of the filter window.

Each filtration stage intricately refines the ECG signal, progressively reducing noise and enhancing signal quality. This meticulous process ensures that each Intrinsic Mode Function (IMF) is optimally processed, leveraging the strengths of Chebyshev Type II, Butterworth, Daubechies Wavelet, and Savitzky-Golay filters. Upon completion of these stages, the IMFs are reassembled to form a composite signal. This reconstructed signal represents a significantly denoised version of the original ECG, retaining critical diagnostic features while minimizing artifacts and noise.

5. Bayesian Multi-Objective Optimization of Filter Parameters

Optimizing filter parameters is pivotal for improving the efficacy of our ECG signal processing model. Our primary goal is to maximize noise reduction while preserving the essential diagnostic features of ECG signals. To accomplish this, we employ a Bayesian multi-objective optimization strategy, known for its ability to navigate complex parameter spaces inherent in signal processing tasks. This method excels in balancing signal fidelity and noise reduction.

5.1. Optimization Process

The optimization process is depicted in Figure 3, which illustrates the sequential application of filters to the intrinsic mode functions (IMFs) extracted from ECG data, culminating in an optimized filtered signal.

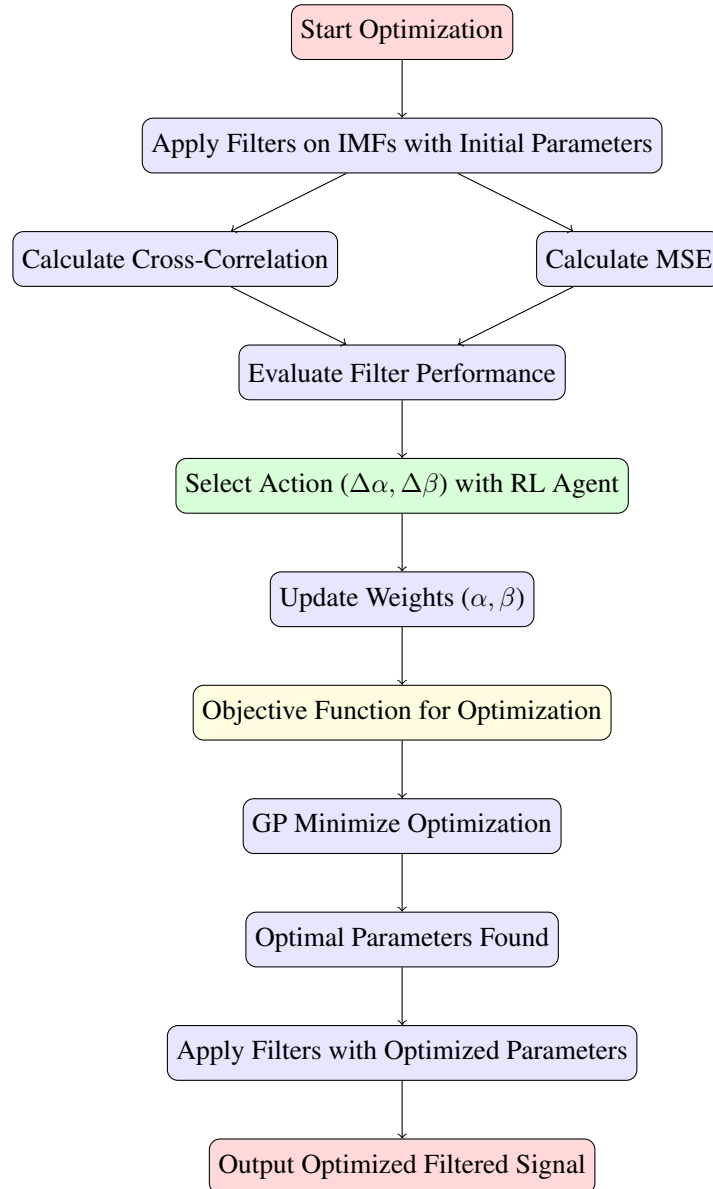


Figure 3. Flowchart showing the Bayesian optimization process with RL-based dynamic weight adjustment for filter parameter tuning in the proposed ECG signal processing model.

5.2. Efficacy Quantification

To quantify the efficacy of the filter application, we compute the cross-correlation and mean squared error (MSE) between the original and filtered signals. Cross-correlation evaluates the preservation of the signal's key characteristics, while MSE measures the deviation from the original signal, indicating the accuracy of the reconstruction.

5.3. Multi-Objective Optimization Approach

Our optimization approach aims to balance the maximization of cross-correlation and the minimization of MSE. We formulate an objective function that incorporates dynamic weights for MSE and cross-correlation, adjusted by a reinforcement learning (RL) agent. The multi-objective optimization process can be mathematically expressed as:

$$\text{minimize } f(\mathbf{x}, \alpha, \beta) = -(\alpha \cdot \text{cc}(\mathbf{x}) - \beta \cdot \text{MSE}(\mathbf{x})), \quad \mathbf{x} \in \mathbf{X}, \quad (6)$$

where α and β are the dynamic weights learned by the RL agent, \mathbf{x} represents the vector of filter parameters to be optimized, and \mathbf{X} defines the feasible domain for these parameters. The terms $\text{cc}(\mathbf{x})$ and $\text{MSE}(\mathbf{x})$ denote the cross-correlation and mean squared error between the original and filtered signals, respectively.

5.4. Reinforcement Learning for Dynamic Weight Adjustment

The RL agent is trained to adjust the weights α and β to optimize the filtering process. The state of the RL environment includes the current values of MSE and cross-correlation, while the action space consists of possible adjustments to α and β .

State:

$$s_t = [\text{MSE}_t, \text{cc}_t, \alpha_t, \beta_t] \quad (7)$$

Action:

$$a_t = [\Delta\alpha_t, \Delta\beta_t] \quad (8)$$

Reward: The reward function encourages the RL agent to maximize cross-correlation and minimize MSE, defined as:

$$r_t = \alpha_t \cdot \text{cc}_t - \beta_t \cdot \text{MSE}_t \quad (9)$$

5.5. Optimization Process

The optimization process involves the following steps:

1. Initialize the RL agent with initial weights α_0 and β_0 .
2. At each iteration, the agent observes the current state s_t and selects an action a_t to adjust the weights.
3. Apply the updated weights α_{t+1} and β_{t+1} to the objective function and compute the new values of MSE and cross-correlation.
4. The agent receives a reward based on the new state and updates its policy accordingly.
5. The process repeats until convergence or a predefined number of iterations is reached.

5.6. Optimization Results

Following optimization using the Gaussian process minimization method, we identified the optimal filter parameters listed in Table 1:

These parameters were determined by maximizing the cross-correlation between the original ECG signal and the filtered signal while minimizing the mean squared error (MSE) between these two signals. This approach ensures that the filtered signal retains the essential characteristics of the original signal while effectively eliminating noise.

The application of these optimized parameters within our model has resulted in high-quality denoised ECG signals, as evidenced by significant improvements in performance metrics such as cross-correlation and MSE. This optimization has thus contributed to improving the reliability and precision of our model for processing and analyzing ECG signals, providing a more effective tool for diagnosing cardiac pathologies.

Parameter	Optimal Value
Chebyshev Type II and Butterworth Low Cut Frequency	0.973 Hz
Chebyshev Type II and Butterworth High Cut Frequency	62 Hz
Daubechies Level of Decomposition	7
Savitzky-Golay Window Length	5
Savitzky-Golay Polynomial Order	4

Table 1. Optimal filter parameters for ECG signal processing.

5.7. Performance Metrics Evaluation

To assess the effectiveness of our optimized filter parameters, we compared the performance metrics of the ECG signal processed with default parameters and with the optimized parameters:

Metric	Unoptimized	Optimized
Cross-Correlation	0.858	0.969
MSE	0.307	0.057

Table 2. Comparison of ECG signal filtering performance metrics.

The results in 2 show a significant improvement in both cross-correlation and mean squared error (MSE) with the optimized parameters. The cross-correlation increased from 0.858 in the unoptimized case to 0.964 in the optimized case, indicating a closer resemblance to the original signal. Similarly, the MSE decreased from 0.307 to 0.063, signifying a more effective reduction in noise without major distortion of the original ECG signal. These improvements highlight the efficacy of our optimization approach in enhancing the quality of denoised ECG signals for more accurate diagnostic evaluations.

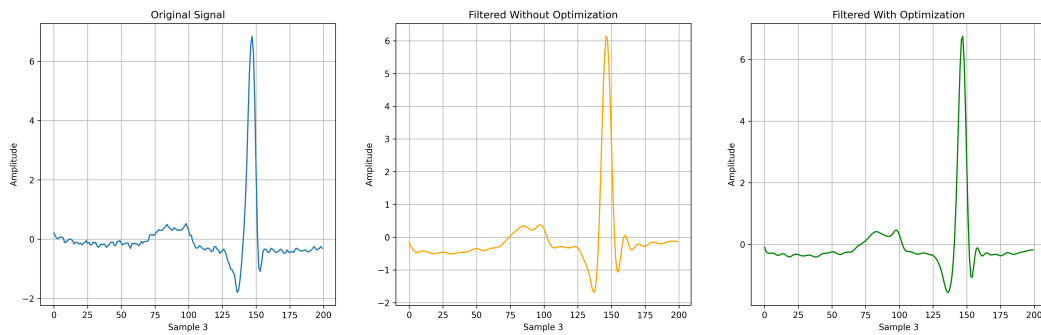
5.8. Signal Visualizations

A crucial aspect of our study is the visualization of ECG signals, essential for assessing the efficacy of the proposed Bayesian multi-objective optimization technique. Figures 4a, 4b, and 4c provide a comparative analysis across different samples, showing the original ECG signal as well as the filtered versions with and without optimization.

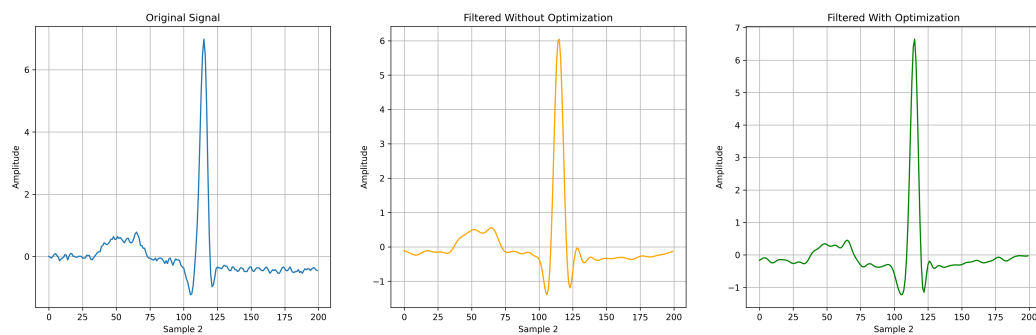
As evidenced in these subfigures 4, the filtered signals without optimization exhibit a reduction in noise compared to the original unfiltered signals. However, the optimized filtered signals show a marked improvement in terms of signal smoothness and the preservation of characteristic waveforms. This is particularly notable in areas where the original signals display pronounced peaks and valleys, highlighting the refinement brought about by the multi-objective optimization process.

These illustrations underscore the proficiency of Bayesian multi-objective optimization in determining the optimal filter parameters, thereby substantiating the practicality and advantages of our proposed method. Such enhancements are imperative for the reliability of ECG signal analysis and its subsequent interpretation by healthcare professionals.

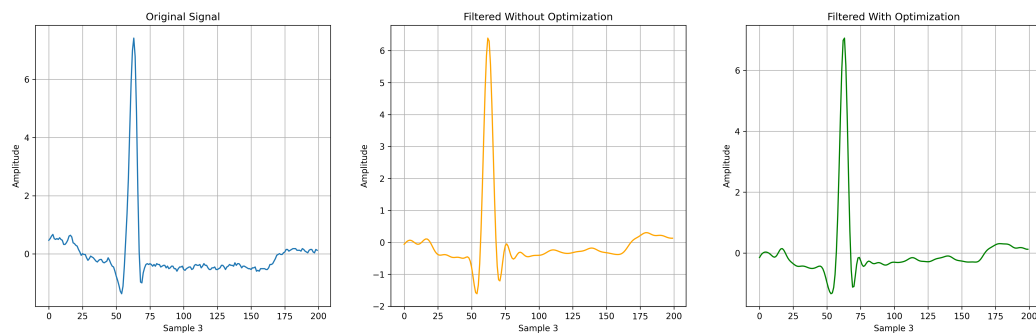
Ultimately, this visual representation not only corroborates the quantitative findings of our multi-objective optimization framework but also provides intuitive insights into the qualitative improvements in ECG signal processing.



(a) Sample 1: Original signal (left), filtered without optimization (middle), filtered with optimization (right).



(b) Sample 2: Original signal (left), filtered without optimization (middle), filtered with optimization (right).



(c) Sample 3: Original signal (left), filtered without optimization (middle), filtered with optimization (right).

Figure 4. Comparative visualization of ECG signals demonstrating the impact of the filtering process with and without Bayesian multi-objective optimization.

6. Proposed Combined Deep Learning Architecture for Classification

The previously described denoising process readies the ECG signals for the critical task of classification. To achieve this, we propose an advanced deep learning architecture designed to identify subtle patterns within the cleaned ECG signals, aiding in the diagnosis of various cardiac conditions, including arrhythmias and myocardial infarction.

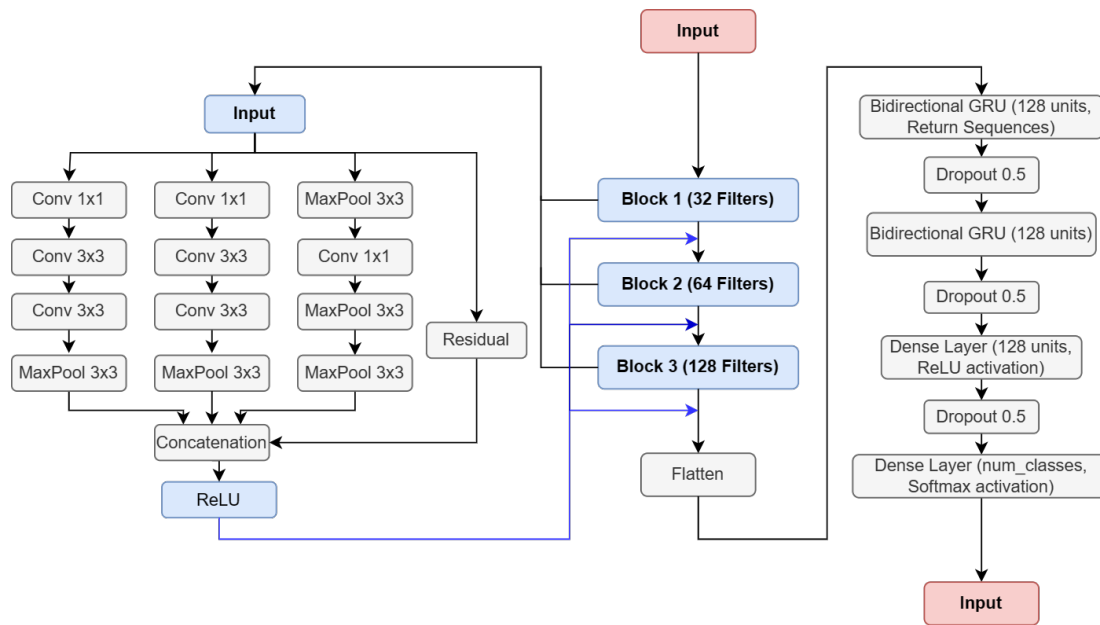


Figure 5. Flowchart showing the proposed combined architecture.

6.1. Architectural Overview

Our proposed architecture, depicted in Figure 5, is composed of multiple interconnected blocks that efficiently and effectively extract features from the input signals. This architecture utilizes parallel processing paths and residual connections to enhance feature representation while maintaining signal integrity. After the feature extraction phase, additional layers further process these features to accurately classify cardiac anomalies.

6.2. Detailed Component Description

The architecture begins with the **Input Layer**, where the raw ECG signal is initially processed. This layer is crucial as it sets the stage for the entire classification process.

Next, we have the **Feature Extraction Block 1**, which employs 32 filters. This block consists of three parallel paths:

- **Path 1:** Includes a 1x1 convolution followed by two 3x3 convolutions.
- **Path 2:** Mirrors Path 1, maintaining a similar structure.
- **Path 3:** Starts with a max pooling layer, followed by a 1x1 convolution and another max pooling layer.

The outputs from these paths are concatenated, and a residual connection is integrated to combine the original input with the concatenated output. This integration helps preserve essential signal information and prevents vanishing gradients. The block concludes with a ReLU activation to add non-linearity.

The second block, **Feature Extraction Block 2**, utilizes 64 filters and follows a similar structure to Block 1. This block captures more complex features from the ECG signals, enhancing the model's ability to detect intricate patterns.

The third block, **Feature Extraction Block 3**, employs 128 filters, following the same structural principles as the previous blocks but with a higher capacity to extract detailed features.

The **Flatten Layer** then transforms the multi-dimensional feature map into a one-dimensional vector, preparing it for further processing.

The architecture proceeds with **Sequential Processing Layers**:

- **Bidirectional GRU (128 units):** Captures temporal dependencies from both directions of the sequence, ensuring a comprehensive understanding of the signal's temporal dynamics.

- A **Dropout layer (0.5)**: Prevents overfitting by randomly dropping units during training.
- This is followed by another **Bidirectional GRU (128 units)**: To further process the temporal features, enhancing the model's ability to detect relevant patterns.

Finally, the model includes **Classification Layers**:

- A **Dense Layer (128 units, ReLU)**: Adds non-linearity and refines the feature representation.
- Another **Dropout layer (0.5)**: Further enhances generalization by preventing overfitting.
- The **Final Dense Layer (Softmax)**: Outputs a probability distribution across different classes of cardiac events for classification.

The **Output Layer** presents the classification results, indicating the detected cardiac conditions based on the processed ECG signal.

6.3. Strategic Use of Architectural Elements

The strategic use of parallel and residual blocks combined with sequential and classification layers allows our architecture to effectively capture both spatial and temporal features. This comprehensive approach ensures accurate classification of ECG signals across various cardiac conditions, providing valuable insights for medical diagnosis and treatment.

By integrating advanced feature extraction techniques and robust classification layers, our proposed architecture stands out in its ability to deliver precise and reliable diagnostics. This significantly enhances the utility of ECG signal analysis in clinical settings, potentially leading to better patient outcomes through more accurate and timely diagnoses.

7. Results and Discussion

The performance of the proposed model was rigorously evaluated for the classification of cardiac arrhythmias (CA) using 12 different ECG leads. The results, summarized in Table 3, highlight the significant improvements achieved through the application of the hybrid filter and multi-criteria Bayesian optimization. These enhancements are evident across all evaluated metrics: classification accuracy (ACC), sensitivity (SNS), and F1 score.

7.1. Comparative Analysis

Table 3 provides a comparative analysis of the model's performance under three different scenarios: without filtration, without optimization, and with optimization. The optimized model consistently outperforms the other configurations across all ECG leads, demonstrating the effectiveness of the proposed approach.

The results clearly indicate the superior performance of the optimized model. Specifically:

- **Accuracy (ACC)**: The model with optimization achieves higher accuracy across all leads compared to the models without filtration and without optimization. For instance, lead I shows an accuracy improvement from 97.63% (without filtration) and 98.02% (without optimization) to 98.85% (with optimization).
- **Sensitivity (SNS)**: The optimized model demonstrates enhanced sensitivity, indicating a better ability to correctly identify true positives. Lead II, for example, shows an increase from 97.63% (without filtration) and 98.03% (without optimization) to 99.04% (with optimization).
- **F1-Score (F1)**: The F1 score, which balances precision and recall, also sees significant improvements with optimization. Lead VI improves from 97.55% (without filtration) and 98.12% (without optimization) to 99.05% (with optimization).

7.2. Visual Analysis of Performance

The following figures provide a visual comparative analysis of the model's performance under three different scenarios: without filtration, without optimization, and with optimization.

Table 3. Comparative performance analysis of the proposed model over 12 ECG leads for Cardiac Arrhythmia classification.

Lead	Without Filtration			Without Optimization			With Optimization		
	ACC (%)	SNS (%)	F1 (%)	ACC (%)	SNS (%)	F1 (%)	ACC (%)	SNS (%)	F1 (%)
I	97.63	97.40	97.30	98.02	98.04	98.83	98.85	98.17	98.70
II	97.57	97.63	97.44	97.95	98.03	97.70	98.47	99.04	98.98
III	96.99	96.91	97.05	98.45	98.25	98.74	98.63	98.41	98.72
V1	97.86	98.24	97.55	98.01	98.03	98.12	98.61	98.53	99.05
V2	97.82	97.81	97.50	97.89	97.84	97.69	98.65	98.34	98.66
V3	96.94	97.01	96.95	97.83	97.81	98.06	98.18	98.35	98.08
V4	96.92	97.20	97.09	98.04	97.96	98.25	98.19	98.70	98.74
V5	96.63	96.66	96.93	97.24	97.37	97.69	98.20	98.24	98.24
V6	96.84	96.78	96.94	97.09	97.20	97.18	98.23	98.26	98.10
aVL	97.17	97.18	97.30	98.58	99.03	99.01	98.86	99.24	99.17
aVR	96.91	96.96	97.00	97.52	97.93	97.83	98.52	98.65	98.20
aVF	96.74	96.92	96.84	97.41	97.50	97.58	98.08	98.02	98.32

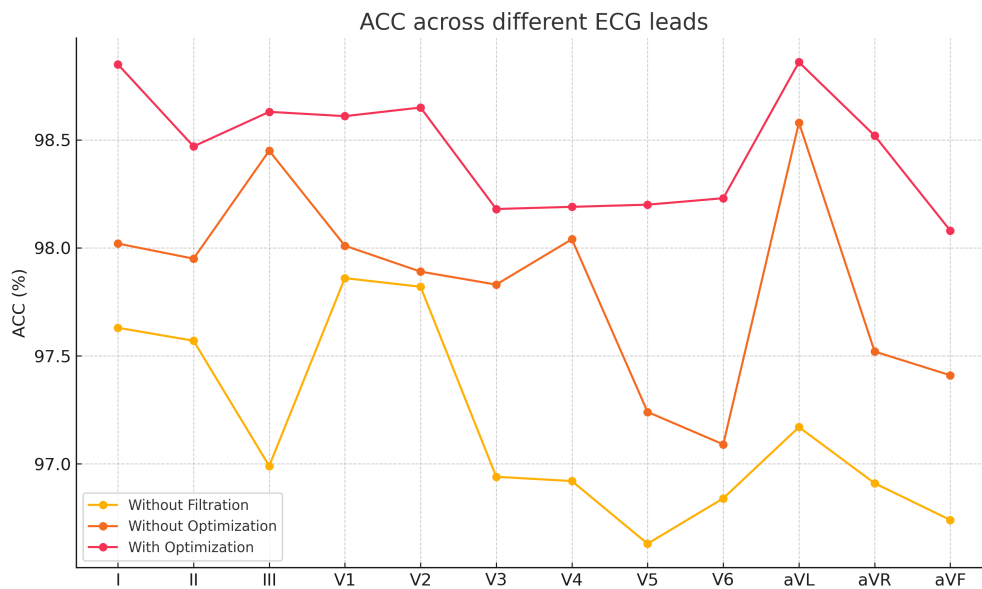


Figure 6. ACC across different ECG leads.

This graph 6 shows the accuracy (ACC) of the model across different ECG leads. It compares three scenarios: without filtration, without optimization, and with optimization. The results demonstrate that optimization significantly enhances the accuracy of cardiac arrhythmia classification for each ECG lead.

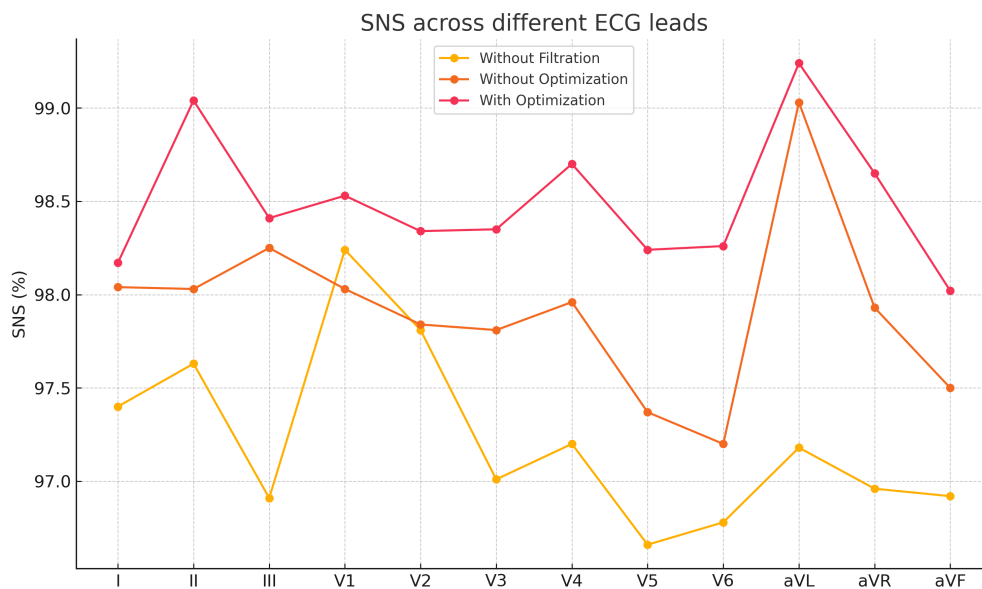


Figure 7. SNS across different ECG leads.

This graph 7 illustrates the sensitivity (SNS) of the model for different ECG leads. It compares the model’s performance without filtration, without optimization, and with optimization. Sensitivity, which measures the model’s ability to correctly identify true positives, is markedly improved after optimization.

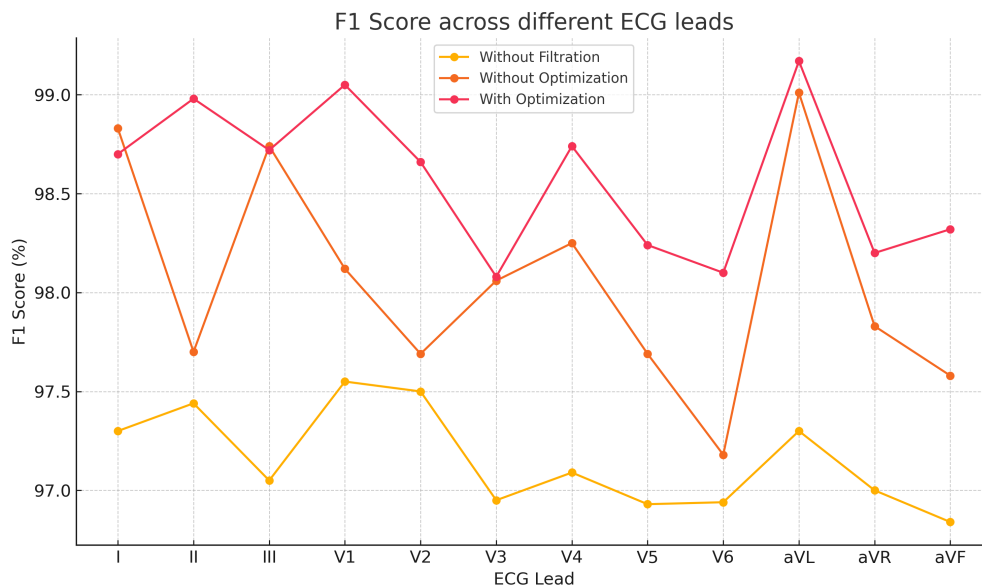


Figure 8. F1 Score across different ECG leads.

This graph 8 presents the F1 score of the model across various ECG leads. The F1 score, which is the harmonic mean of precision and sensitivity, is compared for three scenarios: without filtration, without optimization, and with optimization. Optimization leads to a notable increase in the F1 score for each ECG lead.

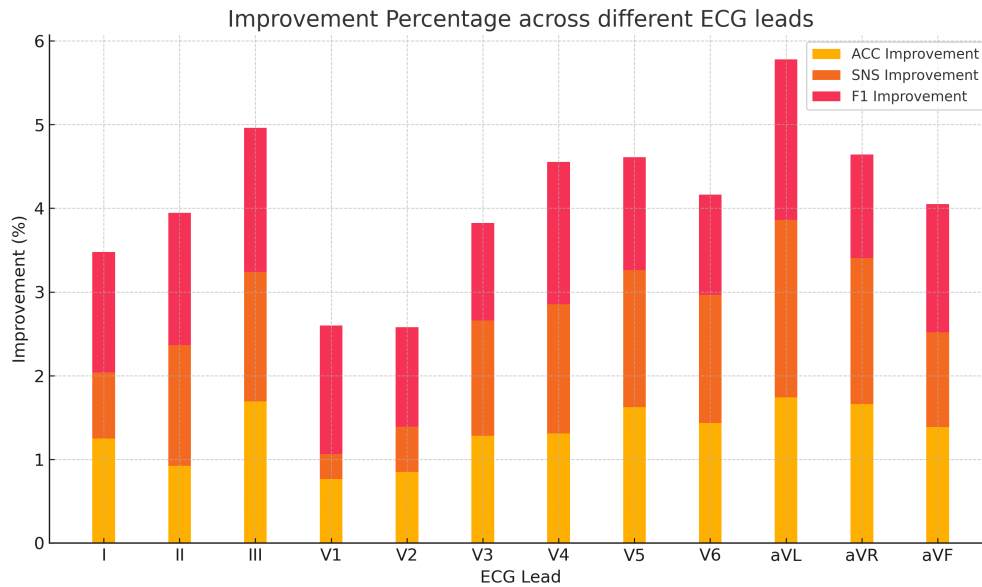


Figure 9. Comparative Improvement Percentage across different ECG leads.

This graph 9 shows the percentage improvement in accuracy (ACC), sensitivity (SNS), and F1 score after optimization compared to the values without filtration. The stacked bars represent the cumulative improvements for each ECG lead. This graph highlights the significant gains achieved through the proposed filtering and optimization techniques.

7.3. Ablation Study

To evaluate the individual impact of each component in our proposed method, we performed an ablation study where we systematically removed each module—Enhanced Empirical Mode Decomposition (EEMD), Chebyshev Type II filter, Butterworth filter, Daubechies Wavelet filter, and Savitzky-Golay filter—from the signal processing pipeline. This approach allowed us to observe how the absence of each module affects critical performance metrics: classification accuracy (ACC), mean squared error (MSE), cross-correlation (CC), and processing time. The results of these experiments are summarized in Table 4.

Table 4. Ablation Study Results: Impact of Removing Each Module on Performance Metrics and Processing Time

Removed Module	ACC (%)	MSE	CC	Time (s)
Without EEMD	86.49	0.1455	0.8118	9.20
Without Chebyshev Type II Filter	92.52	0.0882	0.8910	22.83
Without Butterworth Filter	91.30	0.0842	0.9016	24.35
Without Daubechies Wavelet Filter	91.45	0.0735	0.9207	22.28
Without Savitzky-Golay Filter	94.23	0.0679	0.9405	27.53
Baseline (All Modules)	97.05	0.0617	0.9544	29.39

The ablation results highlight the crucial role each module plays in enhancing the model’s performance, as well as the balance between computational efficiency and processing time:

- **EEMD Removal:** Omitting the EEMD module led to a significant drop in ACC to 86.49%, an increase in MSE to 0.1455, and a decrease in CC to 0.8118. Although the processing time was reduced by approximately 69% (down to 9.20 seconds) due to the computationally intensive nature of EEMD, the substantial decline in performance metrics indicates that EEMD is essential for effectively handling the ECG signal’s non-linear and non-stationary characteristics.

- **Chebyshev Type II Filter Removal:** Excluding this filter resulted in ACC decreasing to 92.52%, MSE increasing to 0.0882, and CC dropping to 0.8910. The processing time was reduced by about 22% to 22.83 seconds. This suggests that the Chebyshev Type II filter plays a significant role in attenuating specific frequency components and enhancing signal fidelity, despite its added computational load.
- **Butterworth Filter Removal:** When the Butterworth filter was removed, ACC declined to 91.30%, MSE rose to 0.0842, and CC decreased to 0.9016. The processing time saw a reduction of around 17%, totaling 24.35 seconds. These results emphasize the importance of the Butterworth filter in minimizing signal distortions and contributing to overall classification accuracy.
- **Daubechies Wavelet Filter Removal:** Eliminating the Daubechies Wavelet filter led to ACC dropping to 91.45%, an MSE of 0.0735, and CC decreasing to 0.9207. The processing time was reduced by approximately 24% to 22.28 seconds. Despite the gain in computational efficiency, the performance loss underscores the filter's vital role in capturing the ECG signal's non-stationary features.
- **Savitzky-Golay Filter Removal:** Removing the Savitzky-Golay filter resulted in a slight decrease in ACC to 94.23%, an increase in MSE to 0.0679, and a reduction in CC to 0.9405. The processing time decreased marginally by about 6% to 27.53 seconds. While this filter adds minimal computational overhead, its contribution to smoothing the signal and improving classification performance is notable.

Overall, the inclusion of all modules yields the best performance, with an ACC of 97.05%, MSE of 0.0617, and CC of 0.9544. The ablation study clearly demonstrates that each component significantly enhances the denoising and classification capabilities of the model. Although some modules contribute to increased processing time, their impact on improving signal quality and accuracy justifies their inclusion in the pipeline.

7.4. Comparative Analysis with State-of-the-Art Methods

To evaluate the effectiveness of our proposed method in ECG signal denoising and arrhythmia classification, we compared it with several recent state-of-the-art techniques. Table 5 presents a summary of these methods, highlighting the denoising strategies, classification models used, and their respective accuracies. Each method employs different approaches, resulting in varying performance levels. Our method achieved a classification accuracy of 99.17%, surpassing other techniques. It is important to note that we could not find sufficient references for a direct comparison that integrates both denoising and classification. Consequently, the comparison here is based on arrhythmia classification using the MIT-BIH Arrhythmia Database—the same dataset utilized in our study.

Table 5. Comparison of our proposed method with state-of-the-art techniques for ECG denoising and classification, showcasing the superior accuracy achieved by our model.

Reference	Denoising Method	Dataset	Classification Model	Accuracy (%)
Murawwat et al. (2022) [66]	Multivariate Empirical Mode Decomposition (MEMD)	MIT-BIH Database Arrhythmia	Artificial Neural Network (ANN)	89.8
Zeng et al. (2023) [68]	Tunable Q-factor Wavelet Transform (TQWT) + Complete Ensemble Empirical Mode Decomposition (CEEMD)	MIT-BIH Database Arrhythmia	CNN + LSTM	97.20
Xia et al. (2023) [67]	Denoising Autoencoder	MIT-BIH Database Arrhythmia	Transformer + CNN	97.93
Singh et al. (2022) [65]	Attention-based Convolutional Denoising Autoencoder (ACDAE)	MIT-BIH Database Arrhythmia	Convolutional Neural Network (CNN)	98.88
Our proposed method	Hybrid Filter: EEMD, Chebyshev Type II, Butterworth, Daubechies Wavelet, Savitzky-Golay Filters	MIT-BIH Database Arrhythmia	Residual and Parallel Deep Learning Architecture	99.17

As shown in Table 5, our method achieves the highest classification accuracy among the compared techniques. This superior performance underscores the effectiveness of our hybrid filtering approach, which combines multiple filters to enhance denoising, along with our advanced deep learning architecture. The integration of these

components contributes to more accurate and reliable arrhythmia classification. These results demonstrate the potential of our method to improve diagnostic accuracy in clinical settings.

7.5. Dataset-Specific Performance and Limitations

Our optimized hybrid filter exhibited substantial enhancements in signal quality and classification performance across several datasets:

- **MIT-BIH Arrhythmia Database [69] and PTB Diagnostic ECG Database [70]:** The filter significantly improved the ECG signals in these datasets, which are known for their standard noise profiles. This demonstrates the filter's effectiveness in handling typical noise characteristics found in clinical ECG recordings.
- **QT Database:** Applied to the QT Database [71], the filter performed effectively across all 12 ECG leads. We observed an average improvement of 1.56% in classification accuracy when comparing the original signals to the filtered ones, and an additional improvement of 1.79% between the filtered and optimized signals. These results underscore the efficacy of our filtering and optimization processes in enhancing ECG signal classification.
- **MIMIC-III Waveform Database:** Conversely, the filter's performance was less satisfactory on the MIMIC-III Waveform Database [72], which contains ECG signals with a high degree of non-stationary noise. This dataset includes recordings from intensive care units, where signals are frequently contaminated by artifacts due to patient movements, interference from medical devices, and ongoing medical interventions. The abrupt and unpredictable variations in noise present significant challenges for our current filtering method.

The primary limitation of our denoising approach, particularly evident with datasets like MIMIC-III, is:

- **Challenges with Highly Non-Stationary Noise:** While EEMD is designed to handle non-stationary signals, it may struggle with noise that is extremely erratic or complex, as seen in the MIMIC-III dataset. The rapid and unpredictable changes in noise patterns can impede the model's ability to effectively decompose and filter out the noise components.

8. Conclusion

This paper presented an advanced ECG signal processing model that combines multi-objective Bayesian optimization with sophisticated filtration and deep learning techniques to enhance classification accuracy. The integration of Enhanced Empirical Mode Decomposition (EEMD) with a sequence of advanced filters—Chebyshev Type II, Butterworth, Daubechies Wavelet, and Savitzky-Golay—proved highly effective in reducing noise while preserving critical signal characteristics. The multi-objective Bayesian optimization strategy, augmented with reinforcement learning for dynamic weight adjustment and Gaussian process minimization, fine-tuned the filter parameters to achieve optimal performance. This approach significantly improved noise reduction and signal fidelity, as evidenced by enhanced cross-correlation and reduced mean squared error metrics.

Subsequently, the optimized signals were processed through a robust combined deep learning architecture, which included feature extraction blocks, sequential processing layers with bidirectional GRUs, and dense classification layers. This architecture demonstrated superior performance in classifying cardiac conditions such as arrhythmias, with notable improvements in accuracy, sensitivity, and F1 score across various ECG leads. Specifically, the highest post-optimization values achieved were 99.24% for accuracy, 99.04% for sensitivity, and 99.05% for F1 score.

Our comprehensive approach highlights the potential of combining advanced signal processing techniques with state-of-the-art optimization and deep learning methods to significantly enhance ECG signal analysis. The results validate the effectiveness of our proposed model in providing reliable and accurate diagnostic tools, thereby contributing to improved patient outcomes in cardiology. This work marks a substantial advancement in the pursuit of high-quality cardiac diagnostics, laying the groundwork for more sophisticated and reliable ECG analysis in clinical practice.

Future research may explore further enhancements by integrating additional machine learning techniques and expanding the dataset to include a broader range of cardiac conditions. Such advancements will continue to refine and improve the accuracy and reliability of ECG signal processing and classification.

Conflicts of interests/Competing interests

The authors declare that they have no conflict of interest.

Funding

This research received no specific grant from any funding agency in the public, commercial, or not-for-profit sectors.

REFERENCES

1. A. Goldberger, L. Amaral, L. Glass, J. Hausdorff, P. Ivanov, R. Mark, J. Mietus, G. Moody, C. Peng, and H. Stanley, *The MIT-BIH Arrhythmia Database*, PhysioBank, MIT, 2000. Disponible à : <https://physionet.org/content/mitdb/1.0.0/>
2. Z. Khatar and D. Bentaleb, *Enhanced ECG Signal Features Transformation to RGB Matrix Imaging for Advanced Deep Learning Classification of Myocardial Infarction and Cardiac Arrhythmia*, Multimedia Tools and Applications, pp. 1–21, 2024, Springer.
3. P. Libby and P. Theroux, *Pathophysiology of Coronary Artery Disease*, Circulation, vol. 111, no. 25, pp. 3481–3488, 2005, American Heart Association.
4. K. Thygesen, J. S. Alpert, A. S. Jaffe, B. R. Chaitman, J. J. Bax, D. A. Morrow, H. D. White, and the Executive Group, *Fourth Universal Definition of Myocardial Infarction (2018)*, Circulation, vol. 138, no. 20, pp. e618–e651, 2018, American Heart Association.
5. G. D. Clifford, C. Liu, B. Moody, L. H. Lehman, I. Silva, Q. Li, A. E. Johnson, and R. G. Mark, *AF Classification from a Short Single Lead ECG Recording: The PhysioNet/Computing in Cardiology Challenge 2017*, In *Proceedings of the 2017 Computing in Cardiology (CinC)*, pp. 1–4, 2017, IEEE.
6. P. Rajpurkar, J. Irvin, R. L. Ball, K. Zhu, B. Yang, H. Mehta, T. Duan, D. Ding, A. Bagul, C. P. Langlotz, et al., *Deep Learning for Chest Radiograph Diagnosis: A Retrospective Comparison of the CheXNeXt Algorithm to Practicing Radiologists*, PLoS Medicine, vol. 15, no. 11, p. e1002686, 2018, Public Library of Science.
7. C. Chauhan, R. K. Tripathy, and M. Agrawal, *Patient Specific Higher Order Tensor Based Approach for the Detection and Localization of Myocardial Infarction Using 12-Lead ECG*, Biomedical Signal Processing and Control, vol. 83, p. 104701, 2023, Elsevier.
8. Q. Sun, C. Liang, T. Chen, B. Ji, R. Liu, L. Wang, M. Tang, Y. Chen, and C. Wang, *Early Detection of Myocardial Ischemia in 12-Lead ECG Using Deterministic Learning and Ensemble Learning*, Computer Methods and Programs in Biomedicine, vol. 226, p. 107124, 2022, Elsevier.
9. Q. Sun, Z. Xu, C. Liang, F. Zhang, J. Li, R. Liu, T. Chen, B. Ji, Y. Chen, and C. Wang, *A Dynamic Learning-Based ECG Feature Extraction Method for Myocardial Infarction Detection*, Physiological Measurement, vol. 43, no. 12, p. 124005, 2023, IOP Publishing.
10. P. D. Barua, E. Aydemir, S. Dogan, M. A. Kobat, F. B. Demir, M. Baygin, T. Tuncer, S. L. Oh, R.-S. Tan, and U. R. Acharya, *Multilevel Hybrid Accurate Handcrafted Model for Myocardial Infarction Classification Using ECG Signals*, International Journal of Machine Learning and Cybernetics, vol. 14, no. 5, pp. 1651–1668, 2023, Springer.
11. C. Han, J. Sun, Y. Bian, W. Que, and L. Shi, *Automated Detection and Localization of Myocardial Infarction with Interpretability Analysis Based on Deep Learning*, IEEE Transactions on Instrumentation and Measurement, vol. 72, pp. 1–12, 2023, IEEE.
12. P. Xiong, S. M.-Y. Lee, and G. Chan, *Deep Learning for Detecting and Locating Myocardial Infarction by Electrocardiogram: A Literature Review*, Frontiers in Cardiovascular Medicine, vol. 9, p. 860032, 2022, Frontiers.
13. W. Pan, Y. An, Y. Guan, and J. Wang, *MCA-Net: A Multi-Task Channel Attention Network for Myocardial Infarction Detection and Location Using 12-Lead ECGs*, Computers in Biology and Medicine, vol. 150, p. 106199, 2022, Elsevier.
14. J. Yu, J. Gao, N. Wang, P. Feng, B. Zhou, and Z. Wang, *Spa-Tem MI: A Spatial-Temporal Network for Detecting and Locating Myocardial Infarction*, IEEE Transactions on Instrumentation and Measurement, 2023, IEEE.
15. V. Jahmunah, E. Y. K. Ng, R.-S. Tan, S. L. Oh, and U. R. Acharya, *Explainable Detection of Myocardial Infarction Using Deep Learning Models with Grad-CAM Technique on ECG Signals*, Computers in Biology and Medicine, vol. 146, p. 105550, 2022, Elsevier.
16. M. Y. Balık, K. Gökçe, S. Atmaca, E. Aslanger, A. Güler, and İ. Öksüz, *Interpretable Deep Learning for Myocardial Infarction Detection from ECG Signals*, In *Proceedings of the 2023 31st Signal Processing and Communications Applications Conference (SIU)*, pp. 1–4, 2023, IEEE.
17. Z. Wang and T. Oates, *Encoding Time Series as Images for Visual Inspection and Classification Using Tiled Convolutional Neural Networks*, In *Workshops at the Twenty-Ninth AAAI Conference on Artificial Intelligence*, vol. 1, 2015, AAAI.

18. Z. Wang, W. Yan, and T. Oates, *Time Series Classification from Scratch with Deep Neural Networks: A Strong Baseline*, In *Proceedings of the 2017 International Joint Conference on Neural Networks (IJCNN)*, pp. 1578–1585, 2017, IEEE.
19. I. Daubechies, *Ten Lectures on Wavelets*, SIAM, 1992.
20. P. S. Addison, *The Illustrated Wavelet Transform Handbook: Introductory Theory and Applications in Science, Engineering, Medicine and Finance*, CRC Press, 2017.
21. W. T. Freeman and E. H. Adelson, *The Design and Use of Steerable Filters*, *IEEE Transactions on Pattern Analysis and Machine Intelligence*, vol. 13, no. 9, pp. 891–906, 1991.
22. K. He, X. Zhang, S. Ren, and J. Sun, *Deep Residual Learning for Image Recognition*, In *Proceedings of the IEEE Conference on Computer Vision and Pattern Recognition*, pp. 770–778, 2016.
23. C. Szegedy, W. Liu, Y. Jia, P. Sermanet, S. Reed, D. Anguelov, D. Erhan, V. Vanhoucke, and A. Rabinovich, *Going Deeper with Convolutions*, In *Proceedings of the IEEE Conference on Computer Vision and Pattern Recognition*, pp. 1–9, 2015.
24. Z. Khatar, D. Bentaleb, and O. Bouattane, *Advanced Detection of Cardiac Arrhythmias Using a Three-Stage CBD Filter and a Multi-Scale Approach in a Combined Deep Learning Model*, *Biomedical Signal Processing and Control*, vol. 88, p. 105551, 2024, Elsevier.
25. A. L. Goldberger, L. A. N. Amaral, L. Glass, J. M. Hausdorff, P. C. Ivanov, R. G. Mark, J. E. Mietus, G. B. Moody, C.-K. Peng, and H. E. Stanley, *PhysioBank, PhysioToolkit, and PhysioNet: Components of a New Research Resource for Complex Physiologic Signals*, *Circulation*, vol. 101, no. 23, pp. e215–e220, 2000, American Heart Association.
26. C. Zhang, M. Jiang, Y. Li, L. Xia, Z. Wang, Y. Wu, Y. Wang, and H. Zhang, *An Efficient ECG Denoising Method by Fusing ECA-Net and CycleGAN*, *Mathematical Biosciences and Engineering*, vol. 20, no. 2, pp. 2023–2041, 2023, American Institute of Mathematical Sciences.
27. B. Hossain, M.-B. Hossain, S. K. Bashar, J. Lázaro, N. Reljin, Y. Noh, and K. H. Chon, *A Robust ECG Denoising Technique Using Variable Frequency Complex Demodulation*, *Computer Methods and Programs in Biomedicine*, vol. 195, p. 105856, 2020, Elsevier.
28. T. Trigano, S. Talala, and D. Luengo, *Adaptive Trend Filtering for ECG Denoising and Delineation*, *IEEE Journal of Biomedical and Health Informatics*, vol. 27, no. 1, pp. 371–380, 2023, IEEE.
29. H. Y. Mir and O. Singh, *Power-Line Interference and Baseline Wander Elimination in ECG Using VMD and EWT*, *Computer Methods in Biomechanics and Biomedical Engineering*, vol. 26, no. 5, pp. 583–594, 2023, Taylor & Francis.
30. F. L. Mvuh, C. O. V. Ko'a Ebode, and B. Bodo, *Multichannel High Noise Level ECG Denoising Based on Adversarial Deep Learning*, *Scientific Reports*, vol. 14, no. 1, p. 801, 2024, Nature Publishing Group.
31. X. Wang, B. Chen, M. Zeng, Y. Wang, H. Liu, R. Liu, L. Tian, and X.-S. Lu, *An ECG Signal Denoising Method Using Conditional Generative Adversarial Net*, *IEEE Journal of Biomedical and Health Informatics*, vol. 26, no. 4, pp. 1753–1762, 2022, IEEE.
32. P. Singh, S. Shah Nawazuddin, and G. Pradhan, *Significance of Modified Empirical Mode Decomposition for ECG Denoising*, In *Proceedings of the Annual International Conference of the IEEE Engineering in Medicine and Biology Society (EMBC)*, pp. 3039–3042, 2017, IEEE.
33. H. Huang, S. Hu, and Y. Sun, *A Discrete Curvature Estimation Based Low-Distortion Adaptive Savitzky–Golay Filter for ECG Denoising*, *Sensors*, vol. 19, no. 7, p. 1617, 2019, MDPI.
34. M. Zhang and W. Guo, *An Integrated EMD Adaptive Threshold Denoising Method for Reduction of Noise in ECG*, *PLoS ONE*, vol. 15, no. 7, p. e0235330, 2020, Public Library of Science.
35. Z. Wang, T. Rades, F. Wan, C. M. Wong, and L. Zhang, *Adaptive Fourier Decomposition Based ECG Denoising*, *Computers in Biology and Medicine*, vol. 77, pp. 195–205, 2016, Elsevier.
36. H. D. Hesar and M. Mohebbi, *An Adaptive Kalman Filter Bank for ECG Denoising*, *IEEE Journal of Biomedical and Health Informatics*, vol. 24, no. 9, pp. 2575–2584, 2020, IEEE.
37. A. Kumar, H. Tomar, V. K. Mehla, R. Komaragiri, and M. Kumar, *Stationary Wavelet Transform Based ECG Signal Denoising Method*, *ISA Transactions*, vol. 107, pp. 247–260, 2020, Elsevier.
38. R. Souriau, J. Fontecave-Jallon, and B. Rivet, *Fetal ECG Denoising Using Dynamic Time Warping Template Subtraction*, In *Proceedings of the Annual International Conference of the IEEE Engineering in Medicine and Biology Society (EMBC)*, pp. 1626–1629, 2022, IEEE.
39. H. Wang, Y. Ma, A. Zhang, D. Lin, Y. Qi, and J. Li, *Deep Convolutional Generative Adversarial Network with LSTM for ECG Denoising*, *Computational and Mathematical Methods in Medicine*, vol. 2023, p. 6737102, 2023, Hindawi.
40. S. Sarafan, H. Vuong, D. Jilani, S. Malhotra, M. P. H. Lau, M. Vishwanath, T. Ghirmai, and H. Cao, *A Novel ECG Denoising Scheme Using the Ensemble Kalman Filter*, In *Proceedings of the Annual International Conference of the IEEE Engineering in Medicine and Biology Society (EMBC)*, pp. 4627–4630, 2022, IEEE.
41. Y. Hou, R. Liu, M. Shu, X. Xie, and C. Chen, *Deep Neural Network Denoising Model Based on Sparse Representation Algorithm for ECG Signal*, *IEEE Transactions on Instrumentation and Measurement*, vol. 72, pp. 1–11, 2023, IEEE.
42. S. Boda, M. Mahadevappa, and P. Dutta, *A Hybrid Method for Removal of Power Line Interference and Baseline Wander in ECG Signals Using EMD and EWT*, *Biomedical Signal Processing and Control*, vol. 66, p. 102466, 2021, Elsevier.
43. N. Mourad, *ECG Denoising Based on Successive Local Filtering*, *Biomedical Signal Processing and Control*, vol. 71, p. 103431, 2022, Elsevier.
44. Z. Huang, S. Yang, Q. Zou, X. Gao, and B. Chen, *A Portable Household Detection System Based on the Combination of Bidirectional LSTM and Residual Block for Automatic Arrhythmia Detection*, *Biomedical Engineering / Biomedizinische Technik*, vol. 68, no. 1, pp. 35–46, 2023, De Gruyter.
45. S. A. Parah, H. Aljuaid, and B. A. Malik, *An Iterative Filtering Based ECG Denoising Using Lifting Wavelet Transform Technique*, *Electronics*, vol. 12, no. 2, p. 387, 2023, MDPI.
46. P. G. Malghan and M. K. Hota, *Grasshopper Optimization Algorithm Based Improved Variational Mode Decomposition Technique for Muscle Artifact Removal in ECG Using Dynamic Time Warping*, *Biomedical Signal Processing and Control*, vol. 71, p. 103437, 2022, Elsevier.
47. A. Timmis, N. Townsend, C. P. Gale, A. Torbica, M. Lettino, S. E. Petersen, E. A. Mossialos, A. P. Maggioni, D. Kazakiewicz, H. T. May, et al., *European Society of Cardiology: Cardiovascular Disease Statistics 2019*, *European Heart Journal*, vol. 41, no. 1, pp.

- 12–85, 2020, Oxford University Press.
48. O. Gaidai, Y. Cao, and S. Loginov, *Global Cardiovascular Diseases Death Rate Prediction*, Current Problems in Cardiology, vol. 48, no. 5, p. 101622, 2023, Elsevier.
 49. D. R. Labarthe, *Epidemiology and Prevention of Cardiovascular Diseases: A Global Challenge*, Jones & Bartlett Publishers, 2010.
 50. S. Chatterjee, R. S. Thakur, R. N. Yadav, L. Gupta, and D. K. Raghuvanshi, *Review of Noise Removal Techniques in ECG Signals*, IET Signal Processing, vol. 14, no. 9, pp. 569–590, 2020, Wiley Online Library.
 51. H. Limaye and V. V. Deshmukh, *ECG Noise Sources and Various Noise Removal Techniques: A Survey*, International Journal of Application or Innovation in Engineering & Management, vol. 5, no. 2, pp. 86–92, 2016.
 52. K. Yu, L. Feng, Y. Chen, M. Wu, Y. Zhang, P. Zhu, W. Chen, Q. Wu, and J. Hao, *Accurate Wavelet Thresholding Method for ECG Signals*, Computers in Biology and Medicine, vol. 169, p. 107835, 2024, Elsevier.
 53. F. L. Mvuh, C. O. V. Ko'a Ebode, and B. Bodo, *Multichannel High Noise Level ECG Denoising Based on Adversarial Deep Learning*, Scientific Reports, vol. 14, no. 1, p. 801, 2024, Nature Publishing Group.
 54. S. Velusamy, G. Thangavel, and M. Z. U. Rahman, *Comprehensive Survey on ECG Signal Denoising, Feature Extraction and Classification Methods for Heart Disease Diagnosis*, In *AIP Conference Proceedings*, vol. 2512, no. 1, 2024, AIP Publishing.
 55. G. A. Roth, G. A. Mensah, C. O. Johnson, G. Addolorato, E. Ammirati, L. M. Baddour, N. C. Barengo, A. Z. Beaton, E. J. Benjamin, C. P. Benziger, et al., *Global Burden of Cardiovascular Diseases and Risk Factors, 1990–2019: Update from the GBD 2019 Study*, Journal of the American College of Cardiology, vol. 76, no. 25, pp. 2982–3021, 2020, Elsevier.
 56. P. Kligfield, L. S. Gettes, J. J. Bailey, R. Childers, B. J. Deal, E. W. Hancock, G. Van Herpen, J. A. Kors, P. Macfarlane, D. M. Mirvis, et al., *Recommendations for the Standardization and Interpretation of the Electrocardiogram: Part I*, Journal of the American College of Cardiology, vol. 49, no. 10, pp. 1109–1127, 2007, Elsevier.
 57. S. Luo and P. Johnston, *A Review of Electrocardiogram Filtering*, Journal of Electrocardiology, vol. 43, no. 6, pp. 486–496, 2010, Elsevier.
 58. Z. Khatar, D. Bentaleb, and M. El Mansouri, *Integrating Advanced Combined Numerical Filters for ECG Denoising and Cardiovascular Disease Classification Using Deep Learning*, In *Proceedings of the International Conference on Digital Technologies and Applications*, pp. 539–547, 2024, Springer.
 59. Y. Liu, L. Yao, and Y. Xu, *Deep Learning for Smart Grid: A Comprehensive Survey*, IEEE Access, vol. 7, pp. 23535–23556, 2018, IEEE.
 60. S. Hong, Y. Zhou, J. Shang, C. Xiao, and J. Sun, *Opportunities and Challenges of Deep Learning Methods for Electrocardiogram Data: A Systematic Review*, Computers in Biology and Medicine, vol. 122, p. 103801, 2020, Elsevier.
 61. A. Mincholé and B. Rodriguez, *Machine Learning in the Electrocardiogram*, Journal of Electrocardiology, vol. 57, pp. S61–S64, 2019, Elsevier.
 62. S. Li, Y. Li, Z. Wang, and C. Yang, *A Novel Approach for ECG Signal Denoising to Remove Motion Artifacts Based on Wavelet Transform and Adaptive Filtering*, Biomedical Signal Processing and Control, vol. 72, p. 103316, 2022, Elsevier.
 63. Z. Zhao, Y. Zhang, Y. Deng, X. Zhang, and N. Zhang, *ECG Signal Denoising Using Variational Mode Decomposition and Correlation Analysis for Wearable Devices*, Sensors, vol. 21, no. 4, p. 1145, 2021, MDPI.
 64. D. Bentaleb and Z. Khatar, *Multi-criteria Bayesian Optimization of Empirical Mode Decomposition and Hybrid Filters Fusion for Enhanced ECG Signal Denoising and Classification: Cardiac Arrhythmia and Myocardial Infarction Cases*, Computers in Biology and Medicine, vol. 184, p. 109462, 2025, Elsevier.
 65. P. Singh and A. Sharma, *Attention-Based Convolutional Denoising Autoencoder for Two-Lead ECG Denoising and Arrhythmia Classification*, IEEE Transactions on Instrumentation and Measurement, vol. 71, pp. 1–10, 2022, IEEE.
 66. S. Murawwat, H. M. Asif, S. Ijaz, M. I. Malik, and K. Raahemifar, *Denoising and Classification of Arrhythmia Using MEMD and ANN*, Alexandria Engineering Journal, vol. 61, no. 4, pp. 2807–2823, 2022, Elsevier.
 67. Y. Xia, Y. Xiong, and K. Wang, *A Transformer Model Blended with CNN and Denoising Autoencoder for Inter-Patient ECG Arrhythmia Classification*, Biomedical Signal Processing and Control, vol. 86, p. 105271, 2023, Elsevier.
 68. W. Zeng, B. Su, Y. Chen, and C. Yuan, *Arrhythmia Detection Using TQWT, CEEMD and Deep CNN-LSTM Neural Networks with ECG Signals*, Multimedia Tools and Applications, vol. 82, no. 19, pp. 29913–29941, 2023, Springer.
 69. A. Goldberger, L. Amaral, L. Glass, J. Hausdorff, P. Ivanov, R. Mark, J. Mietus, G. Moody, C. Peng, and H. Stanley, *The MIT-BIH Arrhythmia Database*, PhysioBank, MIT, 2000. Disponible à : <https://physionet.org/content/mitdb/1.0.0/>
 70. A. L. Goldberger, L. A. N. Amaral, L. Glass, J. M. Hausdorff, P. C. Ivanov, R. G. Mark, J. E. Mietus, G. B. Moody, C.-K. Peng, and H. E. Stanley, *PhysioBank, PhysioToolkit, and PhysioNet: Components of a New Research Resource for Complex Physiologic Signals*, Circulation, vol. 101, no. 23, pp. e215–e220, 2000, American Heart Association.
 71. P. Laguna, R. G. Mark, A. L. Goldberger, and G. B. Moody, *QT Database*, PhysioBank, 1997. Disponible à : <https://physionet.org/content/qtodb/>
 72. G. B. Moody, W. K. Muldrow, and R. G. Mark, *MIMIC-III Waveform Database*, PhysioBank, 1996. Disponible à : <https://physionet.org/content/mimic3wdb/>